Modeling and characterization of exciplexes in photoredox CO_2 reduction: Insights from quantum chemistry and fluorescence spectroscopy

Kareesa J. Kron,[†] Jonathan Ryan Hunt,[‡] Jahan M. Dawlaty,[*,‡] and Shaama Mallikarjun Sharada[*,†,‡]

[†]*Mork Family Department of Chemical Engineering and Materials Science, University of Southern California, Los Angeles, California, 90089, United States*

[‡]*Department of Chemistry, University of Southern California, Los Angeles, California, 90089, United States*

E-mail: dawlaty@usc.edu; ssharada@usc.edu

Abstract

Interactions between excited state arenes and amines can lead to the formation of structures with distinct emission behavior. These excited state complexes or exciplexes can reduce the ability of the arene to participate in other reactions, such as CO_2 reduction, or increase the likelihood of degradation via Birch reduction. Exciplex geometries are necessary to understand photophysical behavior and probe degradation pathways but are challenging to calculate. We establish a detailed computational protocol for calculation, verification, and characterization of exciplexes. Using fluorescence spectroscopy, we first demonstrate the formation of exciplexes between excited state

oligo-(p-phenylene) (OPP), shown to successfully carry out CO_2 reduction, and triethylamine (TEA). Time-dependent density functional theory (TDDFT) is employed to optimize the geometries of these exciplexes, which are validated by comparing both emission energies and their solvatochromism with experiment. Excited state energy decomposition analysis confirms the predominant role played by charge transfer interactions in the red-shift of emissions relative to the isolated excited state OPP*. We find that although the exciplex emission frequency depends strongly on solvent dielectric, the extent of charge separation in an exciplex does not. Our results also suggest that the formation of solvent-separated ionic radical states upon complete electron transfer competes with exciplex formation in higher dielectric solvents, thereby leading to reduced exciplex emission intensities in fluorescence experiments.

Introduction

By accessing highly reactive radical states through photo-induced excitation and quenching, photoredox catalysts have immense potential as sustainable alternatives to otherwise energy-intensive, thermally activated reaction pathways.[1,2] Organic catalysts present the added benefit over their inorganic counterparts of eliminating dependence on heavy metals, such as Ru and Ir, that constitute the most widely studied class of photoredox catalysts.[3–5] Experimental studies demonstrate successful reduction of CO_2 with organic chromophores known as oligo-p-phenylenes (OPPs) to synthesize formate, amino acids, and hydrocarboxylated styrene.[6–8] The proposed photoredox catalytic cycle for this transformation is shown in Figure 1. OPP is excited to singlet OPP* by UV-vis light. Triethylamine (Et_3N or TEA) quenches OPP* by transferring an electron. The quenched radical anion $OPP^{\cdot-}$ is highly reducing and capable of carrying out the otherwise thermally challenging one-electron reduction of CO_2.

Our previous study describes the electron transfer step from anion radical $OPP^{\cdot-}$ to CO_2 using quantum chemistry methods.[9] In addition, we uncovered means by which cat-

alytic activity can be enhanced by increasing the electron-donating character of substituents (described by their Hammett parameters[10]), or R- groups in Figure 1. However, electron transfer rate coefficients do not exhibit an increase with electron-donating character beyond a certain value of substituent electrophilicity. Rate coefficients exhibit a quadratic dependence on electrophilicity, originating in plateauing free energy driving force as R becomes more electron-donating.

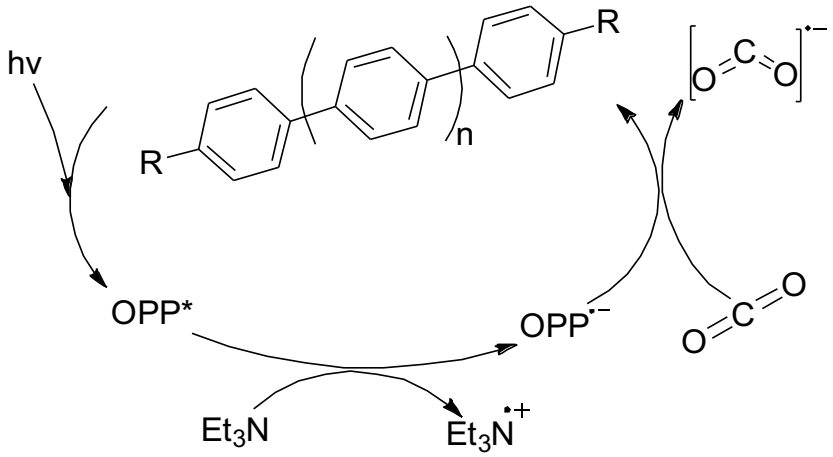

Figure 1: Proposed catalytic cycle of single electron reduction of CO_2 with oligoparaphenylene.[9,11] This study focuses on OPP-3 and OPP-4 where n=1 and 2, respectively, and R = H. Reprinted (adapted) with permission from ref.[9] Copyright 2020 American Chemical Society.

Understanding the CO_2 reduction step alone, however, is not enough to design a viable photoredox pathway. In addition to the inherent complexity associated with light-assisted pathways, experimental studies show that despite high activity towards CO_2 reduction, these chromophores exhibit very low turnover numbers.[6,8] Prior studies attribute this to proton capture and subsequent Birch reduction of the chromophore in the case of OPP and carboxylation in the case of chromophores such as phenanthrene, anthracene, or pyrene.[6,12] It is not yet known at which stage in the photoredox cycle (Figure 1) proton capture occurs or whether the chromophore is in its excited, radical anion, or any other state when capturing a proton.

One possible source of protons is the quenching amine (e.g. TEA) itself, as its α-CH bonds are typically easier to deprotonate compared to similar bonds in an aprotic solvent.[13] While the proton generation from the amine and capture from solution by the arene radical anion can occur as separate steps, simultaneous deprotonation and proton capture may be favorable when the donor-acceptor species are in close proximity. Such encounter complexes between one species in its ground state and another in its excited state, known as excited-state complexes or *exciplexes*, have been reported to form between amines and arenes.[14,15] Exciplexes are identified by their broad, red-shifted fluorescence emission peak relative to that of the isolated excited state chromophore. These emission peaks are distinctly visible in low dielectric solvents and peak intensities are concentration dependent due to the fact that exciplexes are encounter complexes.[16] As exciplexes are proposed to form upon close contact of donor and acceptor species with partial charge transfer between the species,the proton abstraction step of photo-Birch reduction could occur from exciplexes. In other words, the quenching process illustrated in Figure 1[6,11] does not necessarily always lead to distinct radical anion/cation pairs and can instead lead to the formation of exciplexes stabilized by partial charge transfer.

To examine the possibility that degradation is initiated at the exciplex state, one must first calculate the geometry of the exciplex itself. Fluorescence spectroscopy carried out in this study confirms the formation of exciplexes between OPP* and TEA. Quantum chemistry methods are employed to both calculate and characterize the geometries of these exciplexes. We use time-dependent density functional theory (TDDFT) to calculate exciplex geometries formed by OPP-3* and OPP-4* with TEA in solution. The detailed procedure for excited state optimization is presented to serve as a guide for future computational studies. Exciplexes are verified via comparison with experimental fluorescence spectroscopy and solvatochromism and characterized by means of natural transition orbital calculations and excited-state energy decomposition analysis. The broad, red-shifted emission feature associated with an exciplex exhibits both solvatochromic shifts and diminishing intensity with

increasing solvent dielectric in fluorescence experiments.[17,18] In direct contradiction to conventional wisdom, excited-state Mulliken charge analysis reveals that solvent dielectric does not affect donor-acceptor charge distribution in the exciplex, indicating that the ionic character of the exciplex does not vary with solvent dielectric. On the other hand, a comparison of dielectric dependence of exciplex ([OPP-TEA]*) energies with those of contact radical ion pairs (CRIP, $OPP^{\cdot-}$-$TEA^{\cdot+}$) and solvent-separated radical ion pair (SSRIP, $OPP^{\cdot-}$ - - - $TEA^{\cdot+}$) reveals that SSRIPs are energetically more favorable in higher dielectric solvents. Direct formation of SSRIPs from OPP* and TEA therefore competes with the formation of the exciplex in solvents of high dielectric. In summary, this work demonstrates successful computational determination and verification of exciplexes and sheds light on solvent dependence of excited-state quenching processes in arene-amine systems.

Methods

Materials

Para-terphenyl, or the phenylene oligomer consisting of three phenyl groups coordinated in a para-fashion, is referred to as oligo(p-phenylene)-3 or OPP-3, and along similar lines para-quaterphenyl is referred to as OPP-4. OPP-3, OPP-4, triethylamine (TEA), and all solvents are purchased from Sigma Aldrich. All compounds are used without further purification.

Steady-state spectroscopy

Absorption spectra are obtained using a Cary 50 UV-VIS spectrophotometer. Emission spectra are collected on a Jobin-Yvon Fluoromax 5 fluorometer. OPP-3 and OPP-4 solutions of 1×10^{-5} M are used to obtain the steady state spectra in this paper. Measurements are made in a 1 cm fused quartz cuvette.

Computational methods

All simulations are carried out using the *ab initio* quantum chemistry software, Q-Chem version 5.2.1 and above.[19] The conductor-like polarizable continuum model (C-PCM) for implicit solvation[20–22] is employed for all simulations with the exception of excited state energy decomposition analysis. Time-dependent density functional theory (TDDFT)[23,24] is widely used for studying excited state characteristics including exciplexes.[25–29] Practical difficulties associated with the accurate determination of exciplexes on largely shallow potential energy surfaces as well as their characterization, with some exceptions,[25,28,30] are rarely addressed. Unlike ground states, physical intuition cannot guide the generation of a starting guess structure for exciplex calculation. In addition, an exciplex may not be completely represented by a single geometry or electronic structure as is indicated by the broad fluorescence peak in experiments.[14] Using the OPP*-TEA system as a representative exciplex, this work aims to illustrate procedural aspects of the calculation as well as characterization of exciplexes using state-of-the-art quantum chemistry methods for excited states.

Optimization of excited states

Excited states are calculated for both isolated OPP-3 (OPP-3*) and OPP-4 (OPP-4*) as well as the corresponding exciplexes, each in the presence of a single TEA molecule. The starting guess is obtained via geometry optimization in the ground state. We describe the TDDFT/C-PCM excited state optimization[31] protocol in depth as this may serve as a guide to address common operational challenges and high computing costs associated with quantum chemistry studies of excited states.

We do not recommend the use of the low-cost Tamm-Dancoff Approximation (TDA)[32] for exciplex optimizations even though prior studies show that TDA can closely replicate TDDFT values of absorption and emission peaks for large conjugated molecules.[33] This is because a TDDFT calculation of the vertical excitation spectrum of OPP-TEA reveals two states that possess non-negligible oscillator strengths (are optically active). The higher

energy state corresponds to emission out of the excited state of the isolated chromophore, which only weakly interacts with TEA. The second state that is lower in energy corresponds to exciplex emission. TDA fails to identify this critical second state. Therefore, full TDDFT is essential for capturing partial charge transfer states in these arene-amine excited state complexes.

Geometry optimization calculations are first carried out at the B3LYP/6-311G** level of theory[34] with Grimme's D3 dispersion corrections[35–37] and dichloromethane (CH_2Cl_2, DCM) as the representative solvent. As the default stepsize (0.3 a.u.) can result in the pursuit of a state that is different from the exciplex in the course of TDDFT optimization by the state-following method, the stepsize is lowered to 0.02 a.u. The gradient tolerance is also tightened (to 2×10^{-5} a.u.) from its default value (3×10^{-4} a.u.). These restrictions allow us to follow the correct exciplex state at every step and manually restart the optimization if the state-following algorithm begins to follow an incorrect state.

The converged geometries are subjected to a second optimization step at the desired level of theory. Our prior work studying electron transfer from the OPP-$3^{\cdot -}$ radical anion to CO_2 shows that B3LYP can lead to over-delocalization of electron density that directly affects charge transfer characteristics.[38] This over-delocalization is also observable in the exciplex as charge analysis reveals nearly complete charge transfer to the acceptor fragment (-0.93 e) rather than partial charge transfer that is a characteristic feature of the exciplex. To overcome this issue, we utilize the ωB97X-D/def2-TZVP level of theory.[39,40] Table S1 of the SI illustrates differences in ground state and exciplex geometries. We note some changes in exciplex geometry upon re-optimization at the new level of theory. The interfragment distance decreases by 0.16 Å with ωB97X-D and the extent of charge transfer is smaller (-0.64 e) than that observed with B3LYP calculations (Table S2 in SI). We therefore prescribe TDDFT optimization with a tractable level of theory (B3LYP/6-311G**) followed by re-optimization at the desired level to determine the exciplex geometry with reasonable accuracy.

While it is not the primary focus of this study, we note that upon re-optimization of the isolated OPP-3* and OPP-4* excited states with the ωB97X-D/def2-TZVP level of theory, we observe flattening of the acceptor fragment (Table S2 in SI) and reduction in emission energy. This lowering of emission energy stemming from reduced torsional angles between phenyl groups has been reported for similar phenylenes in prior studies.[41] Studies have also suggested that different functionals can lead to different torsion angles and bond lengths for a variety of chromophores and recommend the use of B3LYP followed by single-point calculations at the desired level of theory.[42,43] While partial charge transfer character of the exciplex necessitates the use of ωB97X-D re-optimization, B3LYP optimization may be better suited for identifying isolated OPP-3* and OPP-4* geometries. As discussed in a later section, the dipole moment of ωB97X-D-optimized isolated OPP-3* geometry is very similar to that of the exciplex, unlike the B3LYP-optimized geometry whose dipole moment is almost zero. If the dipole moment of the exciplex and the isolated OPP* are so similar, we would expect to see similar solvatochromic shifts for isolated excited states and exciplexes instead of significantly larger shifts in the latter (Figure 7). Thus, while it is helpful to re-optimize the exciplex geometry at the desired level of theory (ωB97X-D) due to over-delocalization errors arising from B3LYP, it is not necessary or helpful to re-optimize the isolated excited state of OPP*. We therefore carry out single-point calculations of B3LYP-optimized geometries at the desired level of theory for isolated OPP-3* and OPP-4*.

Characterization of Exciplexes

Upon successful convergence of TDDFT geometry optimization, additional steps are necessary to verify that the structure indeed corresponds to an excited state charge transfer complex. Owing to prohibitive computing and memory requirements, Hessian calculations (or vibrational analyses) are not performed to verify that the geometries are minima on the excited state potential energy surface. Instead, we employ both simple model variations as well as sophisticated computational characterization methods to verify and characterize the

exciplex.

To determine components that contribute to OPP-TEA exciplex interactions, we utilize excited state energy decomposition analysis,[30] which we label 'exEDA' to distinguish from ground state EDA methods.[44–47] This technique uses absolutely localized molecular orbitals[48–51] to break down the shift in excitation energy occurring due to exciplex formation from an isolated molecule in its excited state into constituent frozen (Pauli repulsion and electrostatics), polarization, and charge transfer terms. Martin Head-Gordon's group developed and employed exEDA to probe interfragment interactions where one fragment is in its excited state for various excited state dimers (noble gases, arenes), water-charge system, and exciplexes of formamide(halide)-water and pyridine(pyrimidine)-water using ground state and excited state minima, respectively.[30,52] We apply exEDA to the TDDFT-optimized, solvated exciplex geometries to determine the type of underlying interactions that govern emission shifts in exciplexes. We note that exEDA is carried out in the gas phase as the excited state version of EDA that includes solvation is not yet available in Q-Chem.[38]

To further confirm that the stability of the exciplex originates in charge transfer from the nitrogen lone pair in TEA to OPP*, we substitute N with CH in the optimized exciplex geometry. If the structure identified via TDDFT optimization is indeed an exciplex, the (lower energy) peak corresponding to exciplex emission is expected to vanish when N is replaced with CH. In other words, only the (higher energy) peak that is closer in energy to the emission of isolated OPP* is retained. We also generate visual representations of exciplex interactions by means of natural transition orbital (NTO) calculations.[53–55] NTOs are determined for isolated OPP-3*, the [OPP-3-TEA]* exciplex, and OPP-3* complexed with the CH modification of TEA.

To compare with experimental fluorescence spectra, emission energies are calculated using the non-equilibrium PCM solvation model.[56–60] Non-equilibrium PCM enables a realistic representation of the condensed phase system for fast processes such as absorption and fluorescence. To determine vertical emission energies, the energy difference is calculated

between the excited state with its equilibrium solvation shell and the corresponding ground state but without solvent relaxation. As illustrated in Table S3 of the Supporting Information (SI), equilibrium solvation models do not capture experimentally observed solvatochromic shifts in emission spectra for the systems examined here. Emission wavelengths are calculated using both B3LYP/6-311G** and ωB97X-D/def2-TZVP levels of theory. The following solvents are examined – chlorobenzene (PhCl, ϵ = 5.6), bromobenzene (PhBr, ϵ= 5.2), tetrahydrofuran (THF, ϵ = 7.6), diethyl ether (Et_2O, ϵ = 4.3), dibutyl ether (Bu_2O, ϵ = 3.1), ethyl acetate (EtAc, ϵ = 6.0), dichloromethane (DCM, ϵ = 8.9), cyclohexane (cyHex, ϵ = 2.0), and acetonitrile (AN, ϵ = 35.7) – with their respective optical dielectric constants included in the calculation of dielectric response. Calculated emission spectra are contrasted with experiment for isolated OPP-3* and OPP-4* as well as their respective exciplexes, [OPP-3-TEA]* and [OPP-4-TEA]*.

Results and Discussion

Experimental demonstration of exciplex formation

Exciplex fluorescence is found for OPP-3 in cyHex for a range of concentrations of TEA as shown in Figure 2. The red-shifted peaks around 440 nm are broad and increase with increasing concentration of TEA, both of which indicate the formation of encounter complexes with the excited state OPP-3*. Fluorescence of isolated OPP-3* is centered around a wavelength of 345 nm in cyHex. The spectra are consistent with prior studies across various donor-acceptor combinations, which assign the broad or diffuse red-shifted emission relative to the isolated excited state to an exciplex.[14,61] The formation of exciplexes between OPP-3* and TEA across solvents of varying dielectric is shown in Figure 3. Solvatochromism is observed for the exciplex emission peaks with lower energy emissions for higher dielectric solvents.[14] The spectra in both Figures 2 and 3a and 3b are normalized with respect to the maximum intensity of isolated OPP-3* emission so that their spectral features can be

compared.

It is observed that exciplex emission decreases in intensity relative to isolated OPP-3* as the solvent dielectric constant increases, and that emission from the exciplex is no longer observed in solvents with dielectric constants above that of THF (epsilon=7.6). Similar behavior has been observed for a variety of exciplexes in the literature.[17,62–64] The most common explanation for this phenomenon is that the increased efficiency of charge separation in high dielectric solvents decreases the lifetime of the exciplex, and can even favor electron transfer which avoids the exciplex altogether.[62–64] This decrease in lifetime or population of the exciplex results in less emission. The emission is extinguished altogether in sufficiently high dielectric solvents. In a later section, we employ quantum chemistry calculations to show that relative energies of exciplexes and fully charge- and solvent-separated species support this hypothesis. Another possible explanation for decreasing emission intensity in high dielectric solvents is that in high dielectric solvents, the ionic character of the exciplex increases, which decreases the exciplex's radiative rate constant.[17] Computational results (described in a later section) however are in direct contradiction with this possibility as the extent of charge transfer remains about the same across all solvents.

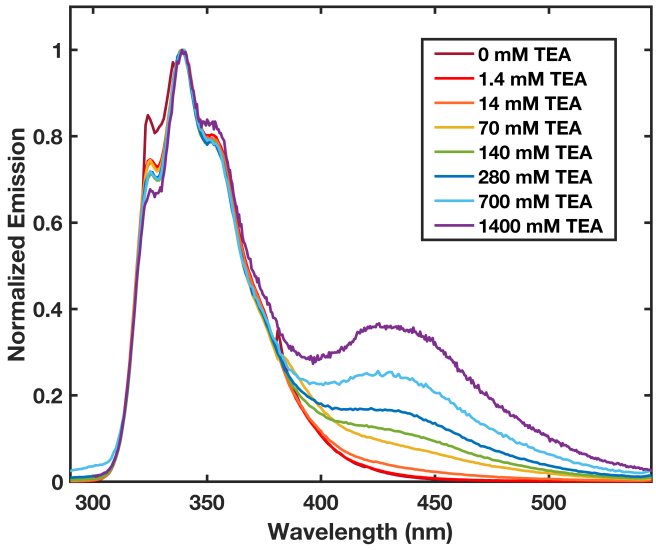

Figure 2: Fluorescence spectra of OPP-3 in cyclohexane in the presence of TEA for various concentrations of TEA.

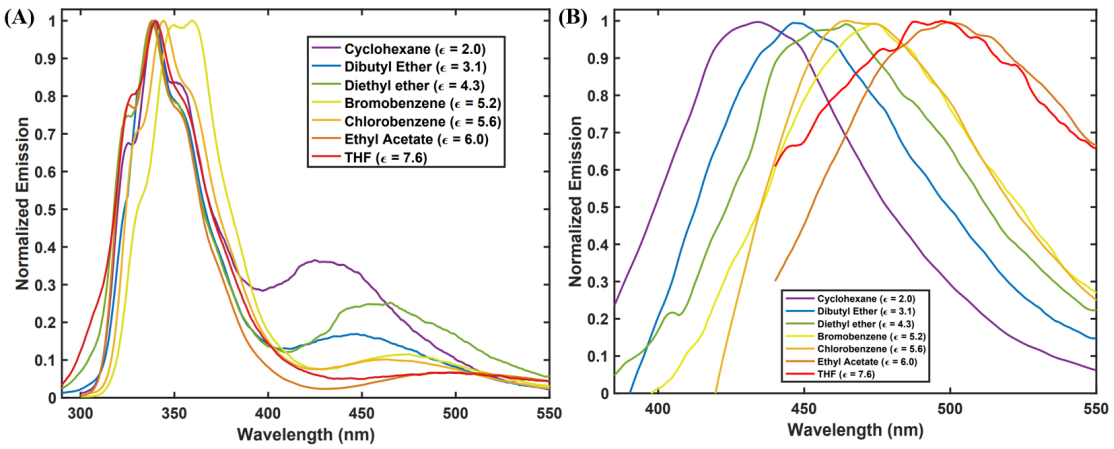

Figure 3: Fluorescence spectra of (A) OPP-3* in the presence of 1.4 M TEA for various solvents and (B) Exciplex emission, normalized for comparison of fluorescence wavelength.

Exciplex features: Geometry and charge transfer

The TDDFT/C-PCM-optimized structures for isolated OPP-3* and the [OPP-3-TEA]* exciplex are shown in Figure 4. Isolated OPP-3* in the relaxed excited state (Figure 4a) has an alternating tilted structure similar to that of the ground state reported in prior studies of oligophenylenes.[9,65,66] Significant structural changes occur in OPP-3* upon interaction with TEA as the phenyl rings in OPP-3* near TEA curve up towards TEA (Figure 4b). As shown in Figure 5, this curvature is also observed in the exciplex formed by OPP-4*. Three of the four phenyl groups in this case create a geometry that closely resembles the [OPP-3-TEA]* exciplex. The fourth phenyl group has a torsional angle that is closer to that of the ground state OPP-4. A visual comparison of the exciplex geometries for the two oligomers suggests that OPP*-TEA interactions are local to the phenyl groups that are closest to TEA.

To determine whether ground state geometries serve as suitable guesses for exciplexes, we compare the geometries of the OPP-3-TEA complex in the ground state (obtained with DFT) with that of the [OPP-3-TEA]* exciplex (TDDFT). Illustrated in Table S1 of the SI, the exciplex state brings the two fragments closer to each other (from 4.08 Å to 3.67 Å between N of the TEA and nearest C−C bond of OPP-3*) and TEA is oriented closer to the

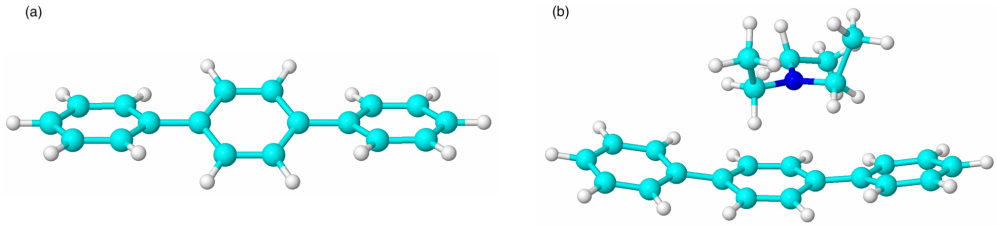

Figure 4: Optimized structures of (a) isolated OPP-3*, and (b) [OPP-3-TEA]* exciplex geometry. C: cyan; H: white; N: blue.

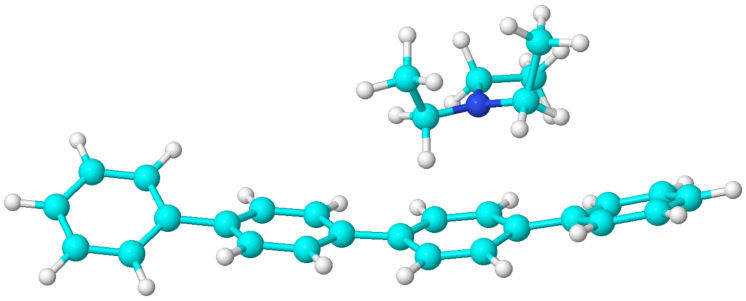

Figure 5: Optimized structure of the [OPP-4-TEA]* exciplex.

middle ring of the phenylene relative to the ground state. In addition, relative phenyl ring orientations are markedly different in the ground and exciplex states. Although TDDFT yields a non-zero oscillator strength, associated with exciplex emission from this ground state geometry, the emission energy is 0.6 eV higher than that obtained with the exciplex geometry and therefore farther away from experiment (Figure 7). Solvated energy decomposition analysis[38] calculations demonstrate that the ground state OPP-3-TEA complex is weakly interacting ($\Delta E_{INT,avg} = -30.4$ kJ/mol) with stabilization dominated by dispersion (Table S4 in SI). Therefore, differences in both structural features and photophysical attributes strongly motivate the use of excited-state optimization methods over ground state approximations to study exciplexes.

A simple control is employed to verify whether the TDDFT-optimized structure is indeed an exciplex. When the N in TEA is replaced with a CH group, the only state with a non-zero oscillator strength corresponds to that of emission from isolated OPP-3*. Disappearance of the red-shifted peak relative to isolated OPP* upon replacing the N in TEA with CH is a

clear indicator that the peak corresponds to interaction of OPP* with the lone pair in the donor. NTOs are contrasted for isolated OPP*, OPP*-TEA, and the CH-modified system, shown in Table S5 of the SI. Each NTO pair is composed of a hole and a particle which reflects the occupied and virtual orbital. The NTO for the exciplex state depicts charge transfer occurring from the lone pair on TEA ('hole') to OPP* ('particle'), serving as proof of formation of an exciplex. NTOs thus serve as further confirmation that the geometry and electronic state identified with TDDFT represent an exciplex and that the emission spectra can be directly contrasted with fluorescence experiments reported in Figure 3.

Origins of exciplex stabilization: Energy decomposition analysis

Energy decomposition analysis of the excited state determines the contribution of frozen, polarization, and charge transfer interactions towards the change in emission energy of the exciplex relative to that of isolated OPP*. The gas phase exEDA results are depicted in Figure 6 for both [OPP-3-TEA]* and its CH-substituted analog. The y-axis represents

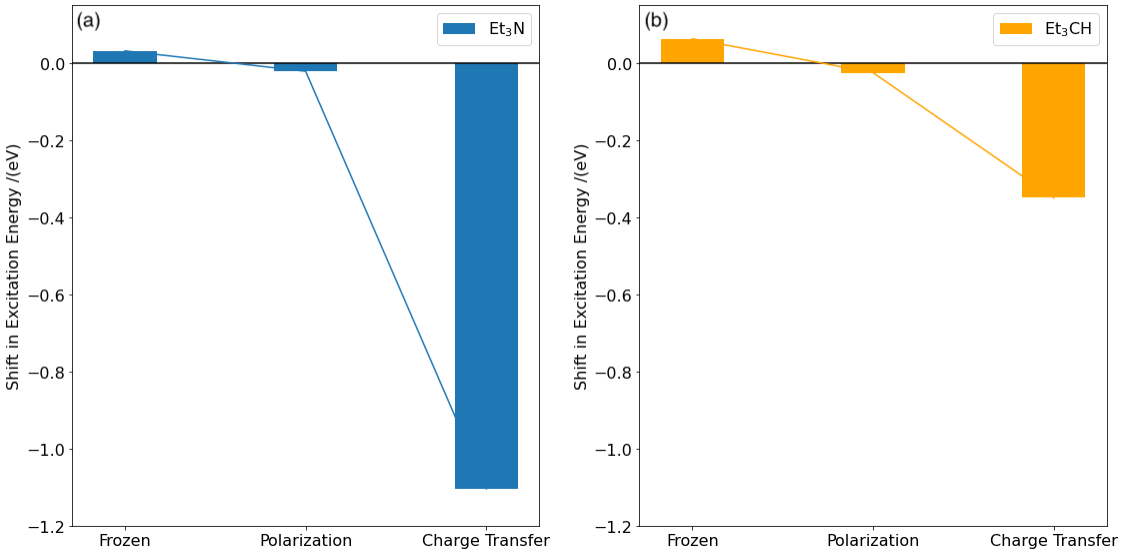

Figure 6: The shifts in emission energies /(eV) of (a) [OPP-3-TEA]* exciplex, and (b) the analog where N in TEA is replaced with CH; with stepwise inclusion of frozen, polarization, and charge transfer interactions obtained using exEDA.

the shift in emission energy of the exciplex referenced to isolated OPP-3*. The [OPP-3-

TEA]* emission energy is increased by a very small amount compared to OPP-3* due to frozen interactions, consisting of electrostatics, dispersion, and Pauli repulsion. Polarization interactions also leads to a negligible shift in emission energy. The biggest shift arises from charge transfer interactions, resulting in 1.10 eV reduction in emission energy. For the CH-substituted control (Figure 6b), the magnitudes of the shifts in emission energy arising from frozen and polarization interactions are also too small (< 0.1eV) to be deemed physically meaningful. Charge transfer interactions in the CH-substituted lead to a 0.35 eV reduction in emission energy. This shift from charge transfer interactions is not observed for the B3LYP-optimized geometry (Figure S1 in SI), consistent with differences in NTOs between B3LYP- and ωB97X-D-optimized geometries. The small extent of charge transfer is likely caused by interaction between the σ orbital of the CH and π^* of OPP due to spatial proximity, which vanishes with increased interfragment separation unlike charge transfer from (N-containing) TEA to OPP. In other words, the (partial) charge transfer-driven shift in emission for [OPP-3-TEA]* is consistent with the prevailing definition of an exciplex and is based on the partial charge transfer from the lone pair of N in TEA. This study does not extend the analysis to probe interactions spanning the entire range of interfragment separations as is often done for excited-state dimers, also known as excimers. The difficulty of studying a range of interfragment separations stems from the asymmetry of the exciplex that makes it challenging to define a single, meaningful coordinate that can capture the range of possible emission energy shifts. The identification of a 'charge transfer coordinate' to examine the impact of interfragment separation on emission energy shifts is therefore a topic for future work.

Exciplex emission & solvatochromism

Experimental emission wavelengths across solvents are contrasted with TDDFT calculations using non-equilibrium solvation for the emission state of isolated OPP* and exciplex emission state of [OPP-TEA]* in Figure 7. The data is also available in Tables S6 and S7 of the SI.

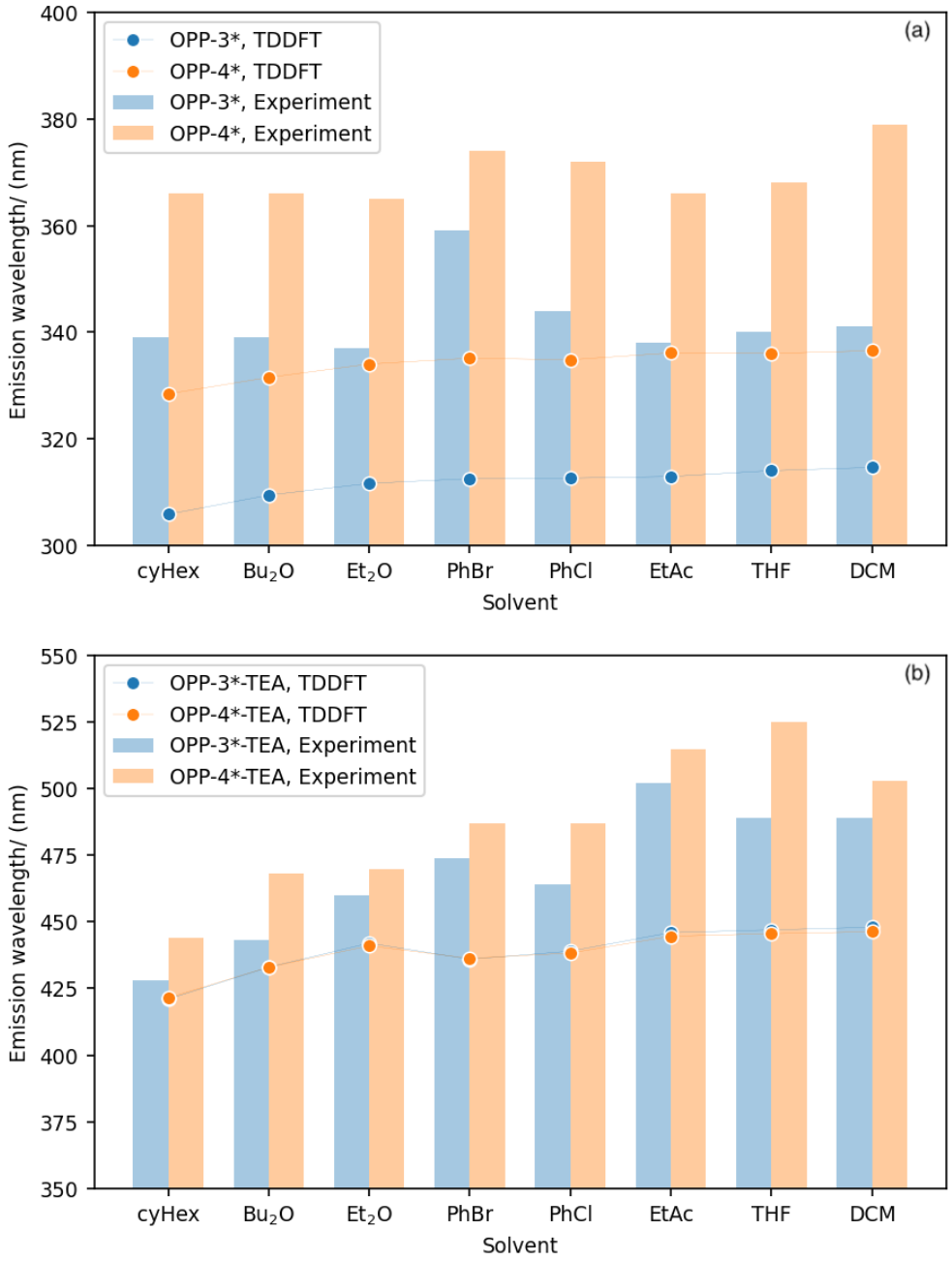

Figure 7: Emission wavelengths for OPP-3 and OPP-4 for (a) isolated catalysts (geometry optimized atB3LYP/6-311G** level of theory), and (b) their exciplex state with TEA (geometry optimized at ωB97X-D/def2-TZVP level of theory). All emission energies are calculated at the ωB97X-D/def2-TZVP level of theory using non-equilibirum solvation.

They show that solvatochromism, or the sensitivity of emission spectra to solvent, is more pronounced for the exciplexes than isolated OPP*. OPP-3* exhibits a very small red-shift in emission wavelength from 339 nm in cyHex ($\epsilon = 2.03$) to 341 nm in THF ($\epsilon = 7.58$), with anomalous red-shifts for aromatic solvents in the middle of this range, specifically PhBr (359 nm) and PhCl (344 nm). The emission maximum in PhBr appears to be associated with a different vibronic feature than in the other solvents, which partially accounts for the large red-shift observed in this solvent. Although we could find no prior evidence to explain this anomalous behavior, we believe that it may be the result of π-stacking interactions between OPP-3* and PhBr (PhCl) solvent molecules. We do not see similarly anomalous behavior for the exciplex in these solvents, possibly because the interaction between OPP-3* and TEA is more favorable than the reaction between OPP-3* and solvent molecules. Experimental emission wavelengths are longer for OPP-4* relative to OPP-3* by, on average, 17 nm. This is because the addition of a phenyl ring to OPP-3 lowers the optical gap of the system owing to extended π-delocalization in the excited state compared to OPP-3*.[66] Similar to OPP-3*, solvatochromic shifts for OPP-4* are small, with the exception of PhBr and PhCl, and emission wavelengths lie in the narrow range of 366-368 nm between cyclohexane and THF.

TDDFT underestimates emission wavelengths (or overestimates energies) for both OPP-3* and OPP-4* by 30 nm (0.35 eV) and 35 nm (0.36 eV) on average, respectively. These deviations from experiment are consistent with blue-shifted wavelengths obtained with hybrid and range-separated hybrid functionals.[42,67–69] The emission spectrum for the control system where N in TEA is replaced with CH does not include the lower energy state corresponding to exciplex emission, thereby verifying that the spectra described in Figure 7b indeed correspond to experimentally observed exciplexes. Computations do not capture the anomalous behavior of exciplexes in PhBr and PhCl as implicit solvation models do not capture specific solute-solvent interactions such as π-stacking. The emission wavelength shifts are small in magnitude but larger than experiment, ranging from 306 nm in cyclohexane to 315 nm in dichloromethane for OPP-3* and 328 nm to 338 nm for OPP-4*.

Experiments (Figures 3 and 7) show that exciplexes emit at longer wavelengths and exhibit more pronounced solvatochromic shifts than isolated OPP*. This difference is because the charge-transfer character of the exciplex results in a much higher ground state dipole moment ($\mu = 0.1184$ Debye) than that of isolated OPP-3* ($\mu = 0.0004$ Debye) and therefore higher sensitivity to solvent environment. The exciplex in EtAc ($\epsilon = 6.02$) is red-shifted by 74 nm and 71 nm relative to cyHex for [OPP-3-TEA]* and [OPP-4-TEA]*, respectively. TDDFT results mirror both the shift relative to isolated OPP* as well as stronger solvatochromic shifts, although the deviations from experiment vary with solvent. Calculated solvatochromic shifts in particular lie in a narrower range when solvent is varied between cyHex and EtAc – 25 nm and 23 nm for [OPP-3-TEA]* and [OPP-4-TEA]*, respectively. Smaller solvatochromic shifts with TDDFT and long range-corrected hybrid functionals have been reported previously for organic heterocyclic dyes.[70] We also compute shifts for a higher dielectric solvent (Table S6 and S7 in SI) where emission from the exciplex is too weak to be observed experimentally, and find that the emission wavelength is 458 nm (455 nm) for [OPP-3-TEA]* ([OPP-4-TEA]*) in AN ($\epsilon = 35.7$). Notably, while the average experimental emission wavelengths are 17 nm higher for [OPP-4-TEA]*, the calculated difference is narrower, 1 nm. In summary, although the differences between calculated and observed emission energies for the exciplex state increase with increasing solvent dielectric, overall trends in calculated and experimental emission spectra are in agreement for both oligomers.

The similarity in TDDFT exciplex emission energies for [OPP-3-TEA]* and [OPP-4-TEA]* mirrors the close resemblance between geometries shown in Figures 4 and 5. Even when the oligomer consists of four phenyl rings, only three interact closely with TEA. As the exciplex electronic state is the result of these localized charge transfer interactions between TEA and OPP*, emission energies are nearly identical across all solvents for the two oligomers. Since broad fluorescence peaks typically indicate that the exciplex is not a unique structure, we examine the range of possible emission energies for [OPP-4-TEA]* resulting from simple rotations of the terminal phenyl ring that is furthest from TEA. The emission

energies resulting from out-of-plane (59.1°) and in-plane torsional rotation (-32.5°) relative to the 'equilibrium' (or minimum energy) geometry are shown in Table S8 of the SI. Rotation of the fourth phenyl out-of-plane leads to on average 7 nm blue-shift in emission energies relative to the in-plane geometry, with the equilibrium emission in between the in-plane and out-of-plane values. Although in-plane rotations lead to [OPP-4-TEA]* emission wavelengths that are slightly higher than [OPP-3-TEA]* across all solvents, the differences are much smaller than experiment (Figure 7). Based on this analysis, we conclude that there are other possible exciplex geometries for [OPP-4-TEA]* that are yet to be identified.

Solvent dependence of exciplex formation

Figure 3 shows that exciplex peak intensities decrease as solvent dielectric increases. This implies that either SSRIPs are formed directly upon complete electron transfer from TEA to OPP* or the exciplex itself has distinct charge transfer characteristics, with greater charge separation favored in higher solvent dielectrics. Gould and coworkers' landmark study addresses this question for exciplexes formed between alkyl-bound benzene donors and cyanoanthracene excited state acceptors using emission quantum yields to calculate efficiencies of exciplex formation in various solvents.[17] They find that exciplexes are formed with unit efficiency in most solvents although the SSRIP can be formed directly if the free energy driving force for complete charge separation and solvation is more favorable relative to exciplex formation.

We first examine the charge distribution in the fragments constituting the exciplex to quantify the extent of charge transfer from TEA to OPP* by varying solvent dielectric but using the exciplex geometry calculated in DCM. The sum of Mulliken atomic charges constituting the OPP-3* fragment in the exciplex electronic state are largely similar across solvents with an average of -0.644 e, ranging from -0.649 e for AN to -0.638 e for PhBr. Reoptimization of the exciplex geometry in a different solvent does not significantly alter the geometry or charge distribution when compared to the reference results with DCM. Within

the constrained search space of exciplex geometries in this study and the approximate continuum treatment of solvent with no explicit involvement of solvent orbitals,[17] we conclude that the extent of charge transfer in an an exciplex state is not sensitive to solvent screening.

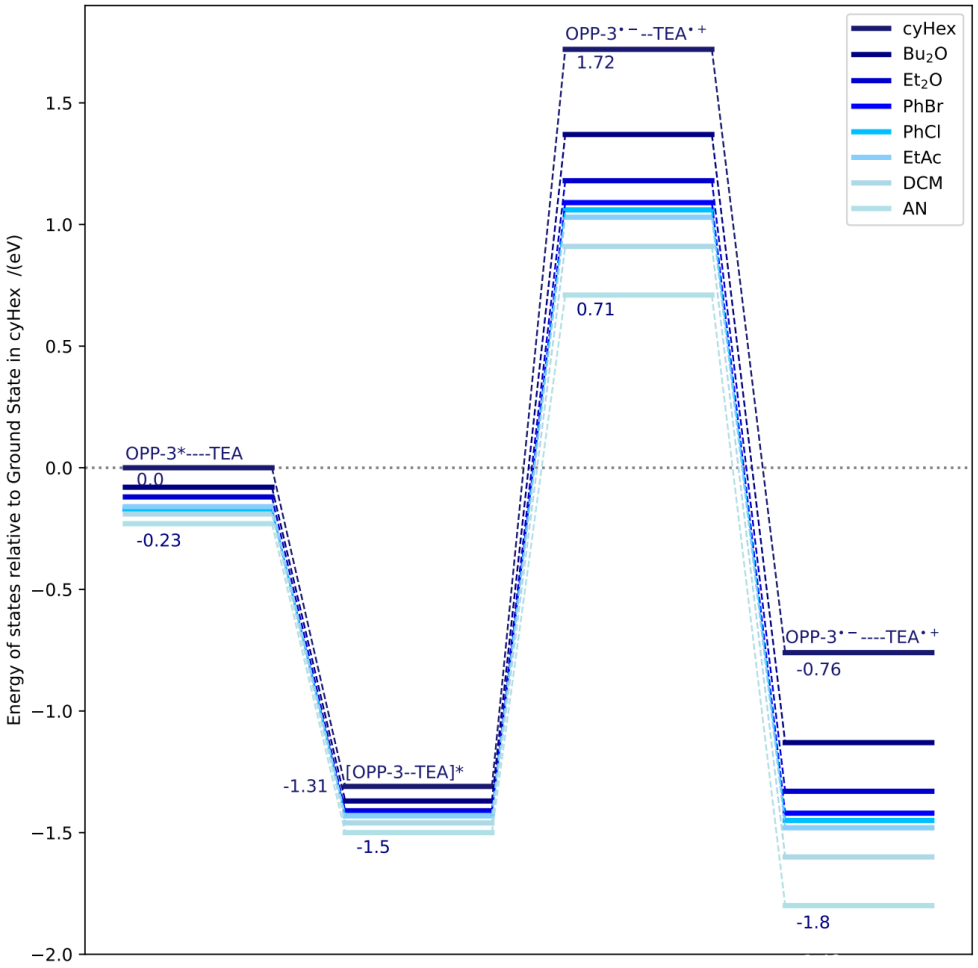

Figure 8: Potential energy surface representing four states (from left to right) – reference state with isolated OPP* and TEA, the exciplex, anionic OPP and cationic TEA radicals at the exciplex geometry (CRIP), and anionic OPP and cationic TEA radicals separated by about 5.5 Å (SSRIP). Dark → light blue indicates increase in solvent dielectric. Energies are reported relative to that of isolated OPP-3* and TEA in cyHex.

We then explore the possibility that SSRIPs are more energetically favorable compared to exciplexes in higher dielectric solvents. Figure 8 depicts the energies of four key states – isolated OPP* and TEA ('OPP-3* - - - TEA'), exciplex state ([OPP-3-TEA]*), CRIP ($OPP\text{-}3^{\cdot-}$-$TEA^{\cdot+}$), and SSRIP ($OPP\text{-}3^{\cdot-}$ - - - $TEA^{\cdot+}$) – relative to a reference isolated

state calculated with cyHex. CRIP energies are calculated at the exciplex geometry using constrained density functional theory (CDFT)[71,72] with the Becke partitioning scheme[73] to isolate the single negative charge on the OPP fragment and positive charge on TEA. SSRIP energies are calculated using CDFT optimization for a system consisting of OPP-3$^{\cdot-}$ and TEA$^{\cdot+}$ that yields a geometry in which the fragments are separated by approximately 5.5 Å. Examination of the kinetics of direct charge transfer from TEA to OPP-3* at this separation to yield an SSRIP is a topic for future work.

Figure 8 shows that the formation of the exciplex from isolated OPP* and TEA is favorable by 1.25-1.3 eV in all solvents. In all cases, imposing complete charge separation on the exciplex geometry leads to a state that is higher in energy than the exciplex. The energy required to form the CRIP in place of the exciplex is highest for the solvent with the lowest dielectric. Higher CRIP energies also mean that charge separation from an exciplex to form SSRIP is associated with a high energetic barrier, and therefore it is more likely that an exciplex is quenched back to a neutral, ground state donor/acceptor pair than to an SSRIP.

Solvent stabilization of the radical ions, or the SSRIP state, lowers the energy relative to CRIP. SSRIPs for low dielectric solvents such as cyHex and Bu_2O are higher in energy compared to the exciplex, indicating that exciplex formation is energetically favored over SSRIP in these solvents. With increasing dielectric, SSRIP formation becomes increasingly favored, implying that this step competes with exciplex formation. Therefore, the decrease in emission intensity with increasing solvent dielectric in Figure 3 can be explained by the fact that excited state quenching to SSRIP becomes more favorable relative to the exciplex state. These observations for arene-amine exciplexes are in complete agreement with experiments for cyanoarene-benzene systems studied by Gould and coworkers.[17] Solvent dielectric therefore does not influence the extent of charge separation in an exciplex state but strongly influences the relative energies of exciplexes and SSRIPs, thereby governing the outcomes of excited state quenching processes.

Conclusions

This work examines the quenching pathways for excited-state OPP* with TEA serving as the sacrificial electron donor by combining fluorescence spectroscopy with a suite of quantum chemistry methods. Experiments confirm the formation of exciplexes, identified by broad, red-shifted emission peaks that decrease in intensity with increasing solvent dielectric. We find that a ground-state donor-acceptor complex is a poor approximation to an exciplex, necessitating the use of excited-state mode-following and optimization methods. TDDFT optimization with tight tolerances and small step-sizes is essential to converge to the correct excited state minimum, an exciplex, in which both charge and excited state are shared by the donor-acceptor complex. Although carrying out a Hessian calculation to verify TDDFT convergence to a minimum can be prohibitive for these systems, we outline techniques that serve to verify and characterize exciplexes. The formation of an exciplex is confirmed by calculating natural transition orbitals, contrasting emission wavelengths and solvatochromism with experiment, and by showing that the emission peak disappears if the N (containing a lone pair) in TEA is replaced with CH. Excited-state energy decomposition analysis shows that donor→acceptor charge transfer is the dominant contributor to the red-shift in emission energy associated with exciplexes. To understand why in experiments lower exciplex emission intensities are observed with increasing solvent dielectric, we determine solvent-dependence of the extent of charge transfer and contrast exciplex energies with those of solvent-separated ion-radical pairs. This analysis reveals that, with increasing solvent dielectric, the extent of charge transfer in an exciplex does not change but SSRIP energy becomes comparable to or lower than the exciplex. We therefore conclude that for these arene-amine systems, SSRIP formation competes with exciplex formation in solvents of higher dielectric, leading to a decrease in observed emission intensities.

Acknowledgement

This material is based upon work supported by the National Science Foundation under Grant No. 2102044. KJK also acknowledges support from the TLARGI Fellowship by USC. JRH and JD were supported by Air Force Office of Scientific Research under AFOSR award FA9550-18-1-0420. The authors are also grateful to USC's Center for Advanced Research Computing for computing resources and technical support.

Supporting Information Available

Supporting information contains the emission wavelengths of the exciplex state calculated with non-equilibrium and equilibrium solvation for several solvents as well as experimental emission energies. Natural transition orbitals are also shown for isolated OPP-3, [OPP-3-TEA]* and the CH-modified system. Cartesian XYZ coordinates for all geometries constituting the potential energy surface are included. Additional analysis of geometric features of both OPP-3 and OPP-4 interacting with TEA is also presented.

References

(1) Shaw, M. H.; Twilton, J.; MacMillan, D. W. Photoredox catalysis in organic chemistry. *The Journal of Organic Chemistry* **2016**, *81*, 6898–6926.

(2) Romero, N. A.; Nicewicz, D. A. Organic photoredox catalysis. *Chemical Reviews* **2016**, *116*, 10075–10166.

(3) Prier, C. K.; Rankic, D. A.; MacMillan, D. W. Visible light photoredox catalysis with transition metal complexes: applications in organic synthesis. *Chemical Reviews* **2013**, *113*, 5322–5363.

(4) Zeitler, K. Photoredox catalysis with visible light. *Angewandte Chemie International Edition* **2009**, *48*, 9785–9789.

(5) Tucker, J. W.; Stephenson, C. R. Shining light on photoredox catalysis: theory and synthetic applications. *The Journal of Organic Chemistry* **2012**, *77*, 1617–1622.

(6) Matsuoka, S.; Ishida, A.; Takamuku, S.; Kusaba, M. Photocatalysis of Ollgo(p-phenylenes). Photochemical Reduction of Carbon Dloxlde with Trlethylamlne. *J. Phys. Chem.* **1992**, *96*, 4437–4442.

(7) Seo, H.; Liu, A.; Jamison, T. F. Direct β-selective hydrocarboxylation of styrenes with CO2 enabled by continuous flow photoredox catalysis. *Journal of the American Chemical Society* **2017**, *139*, 13969–13972.

(8) Seo, H.; Katcher, M. H.; Jamison, T. F. Photoredox activation of carbon dioxide for amino acid synthesis in continuous flow. *Nature Chemistry* **2017**, *9*, 453.

(9) Kron, K. J.; Gomez, S. J.; Mao, Y.; Cave, R. J.; Mallikarjun Sharada, S. Computational Analysis of Electron Transfer Kinetics for CO2 Reduction with Organic Photoredox Catalysts. *Journal of Physical Chemistry A* **2020**, *124*, 5359–5368.

(10) Hammett, L. P. The effect of structure upon the reactions of organic compounds. Benzene derivatives. *Journal of the American Chemical Society* **1937**, *59*, 96–103.

(11) Wada, Y.; Kitamura, T.; Yanagida, S. CO2-fixation into organic carbonyl compounds in visible-light-induced photocatalysis of linear aromatic compounds. *Research on Chemical Intermediates* **2000**, *26*, 153–159.

(12) Tazuke, S.; Kazama, S.; Kitamura, N. Reductive photocarboxylation of aromatic hydrocarbons. *The Journal of Organic Chemistry* **1986**, *51*, 4548–4553.

(13) Barltrop, J. A. The photoreduction of aromatic systems. *Pure and Applied Chemistry* **1973**, *33*, 179–196.

(14) Forster, T. In *The Exciplex*; Gordon, M., Ware, W., Eds.; Academic Press, 1975; pp 1–21.

(15) Weller, A. In *The Exciplex*; Gordon, M., Ware, W., Eds.; Academic Press, 1975; pp 23–38.

(16) Turro, N.; Scaiano, J. C.; Ramamurthy, V. *Principles of Molecular Photochemistry: An Introduction*, 1st ed.; 2009.

(17) Gould, I. R.; Young, R. H.; Mueller, L. J.; Farid, S. Mechanisms of Exciplex Formation. Roles of Superexchange, Solvent Polarity, and Driving Force for Electron Transfer. *Journal of the American Chemical Society* **1994**, *116*, 8176–8187.

(18) Beens, H.; Knibbe, H.; Weller, A. Dipolar Nature of Molecular Complexes Formed in the Excited State. *The Journal of Chemical Physics* **1967**, *47*, 1183–1184.

(19) Epifanovsky, E.; Gilbert, A. T. B.; Feng, X.; Lee, J.; Mao, Y.; Mardirossian, N.; Pokhilko, P.; White, A. F.; Coons, M. P.; Dempwolff, A. L. et al. Software for the frontiers of quantum chemistry: An overview of developments in the Q-Chem 5 package. *The Journal of Chemical Physics* **2021**, *155*, 084801.

(20) Truong, T. N.; Stefanovich, E. V. A new method for incorporating solvent effect into the classical, ab initio molecular orbital and density functional theory frameworks for arbitrary shape cavity. *Chemical Physics Letters* **1995**, *240*, 253 – 260.

(21) Barone, V.; Cossi, M. Quantum Calculation of Molecular Energies and Energy Gradients in Solution by a Conductor Solvent Model. *The Journal of Physical Chemistry A* **1998**, *102*, 1995–2001.

(22) Cossi, M.; Rega, N.; Scalmani, G.; Barone, V. Energies, structures, and electronic properties of molecules in solution with the C-PCM solvation model. *Journal of Computational Chemistry* **2003**, *24*, 669–681.

(23) Casida, M. E. *Recent Advances In Density Functional Methods: (Part I)*; World Scientific, 1995; pp 155–192.

(24) Dreuw, A.; Head-Gordon, M. Single-reference ab initio methods for the calculation of excited states of large molecules. *Chemical Reviews* **2005**, *105*, 4009–4037.

(25) Huenerbein, R.; Grimme, S. Time-dependent density functional study of excimers and exciplexes of organic molecules. *Chemical Physics* **2008**, *343*, 362–371.

(26) Safonov, A. A.; Bagaturyants, A. A.; Sazhnikov, V. A. Assessment of TDDFT- and CIS-based methods for calculating fluorescence spectra of (dibenzoylmethanato)boron difluoride exciplexes with aromatic hydrocarbons. *Journal of Molecular Modeling* **2017**, *23*.

(27) Krueger, R. A.; Blanquart, G. Exciplex Stabilization in Asymmetric Acene Dimers. *Journal of Physical Chemistry A* **2019**, *123*, 1796–1806.

(28) Safonov, A. A.; Bagaturyants, A. A.; Sazhnikov, V. A. Fluorescence Spectra of (Dibenzoylmethanato)boron Difluoride Exciplexes with Aromatic Hydrocarbons: A Theoretical Study. *Journal of Physical Chemistry A* **2015**, *119*, 8182–8187.

(29) Keruckiene, R.; Guzauskas, M.; Lapienyte, L.; Simokaitiene, J.; Volyniuk, D.; Cameron, J.; Skabara, P. J.; Sini, G.; Grazulevicius, J. V. An experimental and theoretical study of exciplex-forming compounds containing trifluorobiphenyl and 3,6-di-: Tert-butylcarbazole units and their performance in OLEDs. *Journal of Materials Chemistry C* **2020**, *8*, 14186–14195.

(30) Ge, Q.; Mao, Y.; Head-Gordon, M. Energy decomposition analysis for exciplexes using absolutely localized molecular orbitals. *Journal of Chemical Physics* **2018**, *148*, 64105.

(31) Liu, J.; Liang, W. Analytical second derivatives of excited-state energy within the

time-dependent density functional theory coupled with a conductor-like polarizable continuum model. *The Journal of Chemical Physics* **2013**, *138*, 024101.

(32) Hirata, S.; Head-Gordon, M. Time-dependent density functional theory within the Tamm-Dancoff approximation. *Chemical Physics Letters* **1999**, *314*, 291–299.

(33) Chantzis, A.; Laurent, A. D.; Adamo, C.; Jacquemin, D. Is the Tamm-Dancoff approximation reliable for the calculation of absorption and fluorescence band shapes? *Journal of Chemical Theory and Computation* **2013**, *9*, 4517–4525.

(34) Becke, A. D. Density-functional thermochemistry. III. The role of exact exchange. *The Journal of Chemical Physics* **1993**, *98*, 5648–5652.

(35) Grimme, S.; Antony, J.; Ehrlich, S.; Krieg, H. A consistent and accurate ab initio parametrization of density functional dispersion correction (DFT-D) for the 94 elements H-Pu. *The Journal of Chemical Physics* **2010**, *132*, 154104.

(36) Grimme, S.; Ehrlich, S.; Goerigk, L. Effect of the damping function in dispersion corrected density functional theory. *Journal of Computational Chemistry* **2011**, *32*, 1456–1465.

(37) Johnson, E. R.; Becke, A. D. A post-Hartree-Fock model of intermolecular interactions: Inclusion of higher-order corrections. *The Journal of Chemical Physics* **2006**, *124*, 174104.

(38) Mao, Y.; Loipersberger, M.; Kron, K. J.; Derrick, J. S.; Chang, C. J.; Sharada, S. M.; Head-Gordon, M. Consistent inclusion of continuum solvation in energy decomposition analysis: theory and application to molecular CO_2 reduction catalysts. *Chemical Science* **2021**, *12*, 1398–1414.

(39) Chai, J.-D.; Head-Gordon, M. Long-range corrected hybrid density functionals with

damped atom-atom dispersion corrections. *Physical Chemistry Chemical Physics* **2008**, *10*, 6615–6620.

(40) Chai, J.-D.; Head-Gordon, M. Systematic optimization of long-range corrected hybrid density functionals. *The Journal of Chemical Physics* **2008**, *128*, 084106.

(41) Panda, A. N.; Plasser, F.; Aquino, A. J.; Burghardt, I.; Lischka, H. Electronically excited states in poly (p-phenylenevinylene): Vertical excitations and torsional potentials from high-level Ab initio calculations. *The Journal of Physical Chemistry A* **2013**, *117*, 2181–2189.

(42) Jacquemin, D.; Planchat, A.; Adamo, C.; Mennucci, B. TD-DFT assessment of functionals for optical 0-0 transitions in solvated dyes. *Journal of Chemical Theory and Computation* **2012**, *8*, 2359–2372.

(43) Wang, J.; Durbeej, B. How accurate are TD-DFT excited-state geometries compared to DFT ground-state geometries? *Journal of Computational Chemistry* **2020**, *41*, 1718–1729.

(44) Horn, P. R.; Head-Gordon, M. Polarization contributions to intermolecular interactions revisited with fragment electric-field response functions. *The Journal of Chemical Physics* **2015**, *143*, 114111.

(45) Horn, P. R.; Head-Gordon, M. Alternative definitions of the frozen energy in energy decomposition analysis of density functional theory calculations. *The Journal of Chemical Physics* **2016**, *144*, 084118.

(46) Horn, P. R.; Mao, Y.; Head-Gordon, M. Defining the contributions of permanent electrostatics, Pauli repulsion, and dispersion in density functional theory calculations of intermolecular interaction energies. *The Journal of Chemical Physics* **2016**, *144*, 114107.

(47) Horn, P. R.; Mao, Y.; Head-Gordon, M. Probing non-covalent interactions with a second generation energy decomposition analysis using absolutely localized molecular orbitals. *Physical Chemistry Chemical Physics* **2016**, *18*, 23067–23079.

(48) Stoll, H.; Wagenblast, G.; Preuβ, H. On the use of local basis sets for localized molecular orbitals. *Theoretica Chimica Acta* **1980**, *57*, 169–178.

(49) Cullen, J. M. An examination of the effects of basis set and charge transfer in hydrogen-bonded dimers with a constrained Hartree–Fock method. *International Journal of Quantum Chemistry* **1991**, *40*, 193–207.

(50) Khaliullin, R. Z.; Head-Gordon, M.; Bell, A. T. An efficient self-consistent field method for large systems of weakly interacting components. *The Journal of Chemical Physics* **2006**, *124*, 204105.

(51) Khaliullin, R. Z.; Bell, A. T.; Head-Gordon, M. Analysis of charge transfer effects in molecular complexes based on absolutely localized molecular orbitals. *The Journal of Chemical Physics* **2008**, *128*, 184112.

(52) Ge, Q.; Head-Gordon, M. Energy decomposition analysis for excimers using absolutely localized molecular orbitals within time-dependent density functional theory and configuration interaction with single excitations. *Journal of Chemical Theory and Computation* **2018**, *14*, 5156–5168.

(53) Martin, R. L. Natural transition orbitals. *Journal of Chemical Physics* **2003**, *118*, 4775–4777.

(54) Luzanov, A. V.; Sukhorukov, A. A.; Umanskii, V. E. Application of transition density matrix for analysis of excited states. *Theoretical and Experimental Chemistry* **1976**, *10*, 354–361.

(55) Mayer, I. Using singular value decomposition for a compact presentation and improved interpretation of the CIS wave functions. *Chemical Physics Letters* **2007**, *437*, 284–286.

(56) Cammi, R.; Tomasi, J. Nonequilibrium solvation theory for the polarizable continuum model: A new formulation at the SCF level with application to the case of the frequency-dependent linear electric response function. *International Journal of Quantum Chemistry* **1995**, *56*, 465–474.

(57) Cossi, M.; Barone, V. Separation between fast and slow polarizations in continuum solvation models. *The Journal of Physical Chemistry A* **2000**, *104*, 10614–10622.

(58) Improta, R.; Barone, V.; Scalmani, G.; Frisch, M. J. A state-specific polarizable continuum model time dependent density functional theory method for excited state calculations in solution. *The Journal of Chemical Physics* **2006**, *125*, 054103.

(59) You, Z.-Q.; Mewes, J.-M.; Dreuw, A.; Herbert, J. M. Comparison of the Marcus and Pekar partitions in the context of non-equilibrium, polarizable-continuum solvation models. *The Journal of Chemical Physics* **2015**, *143*, 204104.

(60) Mewes, J. M.; You, Z. Q.; Wormit, M.; Kriesche, T.; Herbert, J. M.; Dreuw, A. Experimental benchmark data and systematic evaluation of two a posteriori, polarizable-continuum corrections for vertical excitation energies in solution. *Journal of Physical Chemistry A* **2015**, *119*, 5446–5464.

(61) Kavarnos, G. J.; Turro, N. J. Photosensitization by reversible electron transfer: theories, experimental evidence, and examples. *Chemical Reviews* **1986**, *86*, 401–449.

(62) Knibbe, H.; Röllig, K.; Schäfer, F. P.; Weller, A. Charge-Transfer Complex and Solvent-Shared Ion Pair in Fluorescence Quenching. *The Journal of Chemical Physics* **1967**, *47*, 1184–1185.

(63) Knibbe, H.; Rehm, D.; Weller, A. Intermediates and Kinetics of Fluorescence Quenching by Electron Transfer. *Berichte der Bunsengesellschaft für physikalische Chemie* **1968**, *72*, 257–263.

(64) Rehm, D.; Weller, A. Kinetics of Fluorescence Quenching by Electron and H-Atom Transfer. *Israel Journal of Chemistry* **1970**, *8*, 259–271.

(65) Lukeš, V.; Aquino, A. J. A.; Lischka, H.; Kauffmann, H.-F. Dependence of optical properties of oligo-para-phenylenes on torsional modes and chain length. *The Journal of Physical Chemistry B* **2007**, *111*, 7954–7962.

(66) Guiglion, P.; Zwijnenburg, M. A. Contrasting the optical properties of the different isomers of oligophenylene. *Physical Chemistry Chemical Physics* **2015**, *17*, 17854–17863.

(67) Barsuk, I.; Lainé, P. P.; Maurel, F.; Brémond, É. Triangulenium dyes: the comprehensive photo-absorption and emission story of a versatile family of chromophores. *Physical Chemistry Chemical Physics* **2020**, *22*, 20673–20684.

(68) Jacquemin, D.; Perpète, E. A.; Scuseria, G. E.; Ciofini, I.; Adamo, C. TD-DFT performance for the visible absorption spectra of organic dyes: Conventional versus long-range hybrids. *Journal of Chemical Theory and Computation* **2008**, *4*, 123–135.

(69) Jacquemin, D.; Wathelet, V.; Perpète, E. A.; Adamo, C. Extensive TD-DFT benchmark: Singlet-excited states of organic molecules. *Journal of Chemical Theory and Computation* **2009**, *5*, 2420–2435.

(70) Kityk, A. V. Absorption and fluorescence spectra of heterocyclic isomers from long-range-corrected density functional theory in polarizable continuum approach. Journal of Physical Chemistry A. 2012; pp 3048–3055.

(71) Wu, Q.; Van Voorhis, T. Direct optimization method to study constrained systems

within density-functional theory. *Physical Review A - Atomic, Molecular, and Optical Physics* **2005**, *72*.

(72) Wu, Q.; Van Voorhis, T. Constrained density functional theory and its application in long-range electron transfer. *Journal of Chemical Theory and Computation* **2006**, *2*, 765–774.

(73) Becke, A. D. A multicenter numerical integration scheme for polyatomic molecules. *The Journal of Chemical Physics* **1988**, *88*, 2547–2553.

Graphical TOC Entry